SEPERATOR DESIGN CRITERIA FOR A SOLAR-HYDROGEN ELECTROCHEMICAL GENERATOR

S. Haussener[1,2], C. Xiang[3], J. Spurgeon[3], S. Ardon[3], A. Z. Weber[1], N. S. Lewis[3]

[1]Lawrence Berkeley National Laboratory, Berkeley, CA 94720, USA
[2]École Polytechnique Fédéral de Lausanne, Department of Mechanical Engineering, 1015 Lausanne, Switzerland
[3]Beckman Institute and Kavli Nanoscience Institute, California Institute of Technology, Pasadena, CA 91125, USA

Introduction

Solar irradiation is the most abundant energy source available but it is distributed and intermittent, thereby necessitating its storage via conversion to a fuel (e.g., hydrogen). One possible route for direct solar-hydrogen production is through an integrated electrochemical device that uses light-capturing semiconductors in contact with electrodes to generate oxygen and hydrogen [1,2]. Key in such a device is balancing product crossover with Ohmic losses in the solution which necessitate higher photovoltages. Often these requirements are accomplished using a polymer-electrolyte separator [3], yet the exact material-property design targets are not definitively known. In this presentation, a validated multi-physics numerical model of an electrochemical solar-hydrogen generator is used to study its performance. Advantages and limitations concerning current efficiency, required photovoltage, and safety are investigated as a function of separator transport parameters which lead to general design guidelines. Systems including both porous and nonporous photoactive components are examined.

Reactor designs

Three different reactor designs are investigated in the study at hand. Design (i) consists of a multijunction photoactive electrode covered with catalyst on each side [4], (ii) consists of photoanode and photocathode separated by a membrane [5], and (iii) consists of photoelectrodes composed of wire arrays embedded in a proton-conducting membrane [6]. Each of these electrode-separator/membrane-assemblys (ES/MA) is immersed in a conducting water solution. Two-dimensional slices through the design are depicted in figure 1.

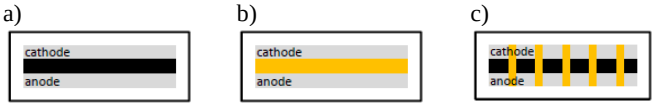

Figure 1. 2D slice through the container of conducting water solution and the ES/MA for designs (i)-(iii) in a)-c). Gray depicts electrodes, orange proton conducing membranes and black a non-conducting support.

Multiphysics model

A multiphysics model is used to examine the tradeoffs and losses in the system. Current and species conservation in the electrolyte and the (porous) electrodes and the (porous) membrane are used as governing equations. The 3D model domain is depicted in figure 2. The electrochemical reactions at the anode and cathode are given by:

$H_2O \rightarrow 1/2O_2 + 2H^+ + 2e^-$,

$2H^+ + 2e^- \rightarrow H_2$,

and are modeled by assuming Butler-Volmer kinetics (exchange current densities at anode and cathode are $1\cdot10^{-7}$A/cm^2 and $1\cdot10^{-3}$A/cm^2, respectively [7]). The assumed boundary conditions are constant current densities at the bottom of the electrode accounting for the produced current of the photoactive components and saturation and zero concentration of the produced species (hydrogen and oxygen) at the cathode and anode, respectively. Therefore any bubble formation and any effect of it on performance are neglected.

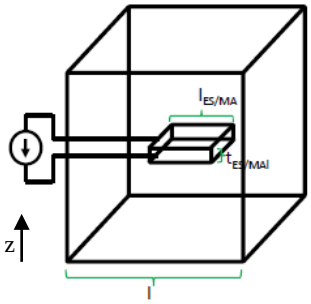

Figure 2. Computational domain for the multi-physics model consisting of a cubic container (edge length l) with immersed ES/MA (edge length $l_{ES/MA}$ and thickness $t_{ES/MA}$).

A measure of the system's performance is the current efficiency, η_i, defined as

$$\eta_i = \frac{1}{V}\int_V \frac{i_v - i_{co}}{i_v} dV$$

where i_{co} is the crossover current given by $i_{co} = \nu F \dot{n}$ (ν: mole number, F: Faraday's constant, $\dot{n}$: molar flux). The Ohmic voltage drop, $\Delta\Phi_R$, in the solution given by the difference of the averaged potential of the liquid or electrolyte, Φ_l, at the two electrodes,

$$\Delta\Phi_R = \frac{1}{V_a}\int_{V_a} \Phi_l dV - \frac{1}{V_c}\int_{V_c} \Phi_l dV \quad ,$$

and is used as an additional performance measure. The operational window for an efficient, cheap and working design is 0.99 current efficiency and 10mV Ohmic drop.

Results

Reference case. Design (i) is chosen as reference case due to its simplicity. The reference parameter for the model are: solution conductivity of 15 S/m (corresponding to 0.5 M H_2SO_4 solution), container edge length of 3 cm, ES/MA edge length of 3 mm and thickness of 100 µm (including two 20 µm electrodes) and electrode conductivity of 10^4 S/m. Convection is neglected. Figure 3 depicts the electrolyte potential and the hydrogen concentration within the container. The reference case shows a current efficiency of 1 and an ohmic drop of 31 mV.

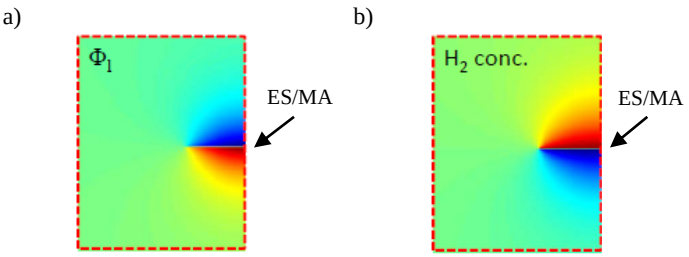

Figure 3. Electrolyte potential (a) and hydrogen concentration (b) in the container for design (i) with the reference parameters along a symmetry plane yz-plane.

Experimental comparison. The calculated ohmic voltage drop over the electrode is compared to experimentally measured drops in

similar systems to validate the model. For the experiment, Pt is evaporated on each side of a glass slide and the sides are electronically connected. Two reference luggin capillary electrodes of Ag/AgCl in glass tubes filled with the same sulfuric-acid electrolyte were prepared. The luggins were positioned at each side of the electrode and measure the potential difference at discrete points for different applied currents. The simulated and measured potential drops are depicted in figure 4. As can be seen, the agreement is good.

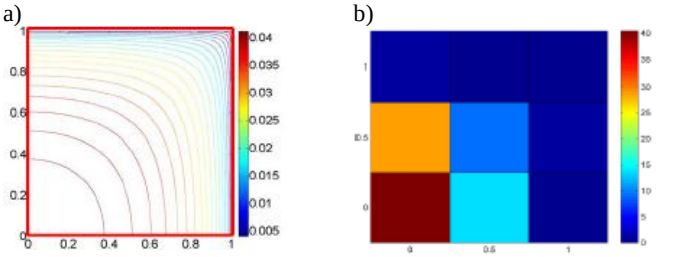

Figure 4. Spatial distribution of Ohmic potential calculated (inV) (a) and experimentally measured (in mV) (b) over one quarter of the electrode.

Geometric optimization. The results for the geometric optimization of the design by means of varying ES/MA length and thickness are depicted in figure 5. Decreasing ES/MA length leads to lower ohmic drops while the current efficiency decreases. The same trend is observed when decreasing thickness of the ES/MA. Design (i) does not allow for operation in the desired operational window.

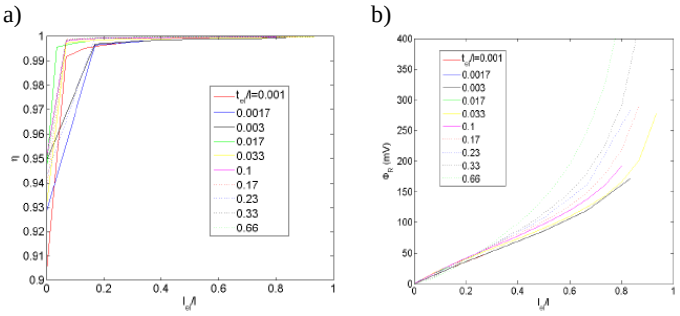

Figure 5. Current efficiency (a) and Ohmic potential drop (b) as function of the container normalized ES/MA length, $l_{ES/MA}/l$, for different container length normalized ES/MA thicknesses, $t_{ES/MA}/l$.

ES/MA design optimization. Performance of design (i) and four variations of design (iii) are depicted in figure 6. The black dot indicates the performance of design (i). Design (iii) without membrane in the pores is one variation (described as D2) of design (iii). Additionally, an inhomogeneous distribution of the pores is investigated. The inhomogeneous case depicted in figure 6 has an ES/MA where the outer edges are the only porous regions (36% of the total surface). The incident current density is linearly decreased with 1−porosity as the surface area is reduced. A porous ES/MA leads to a reduced ohmic drop of one order of magnitude but at the expense of a significant decrease in current efficiency. This decrease can be limited when having an inhomogeneous ES/MA, but such a design only results in a factor of two reduction in the ohmic drop. Design (iii) with a porosity bellow 0.2 allows the device to operate in the desired operational performance window.

Influence of convection. The performance of the devices is substantially decreased when including a convective flow due to pressure gradient that evolves due to the reaction stoichiometry resulting in more hydrogen than oxygen being produced per mole of electrons. Assuming a 1 mbar pressure differential over the device leads to a current efficiency of 0.97 for the reference case (neglecting convection shows current efficiency of 1) while a highly porous electrode leads to a current efficiency of 0.87.

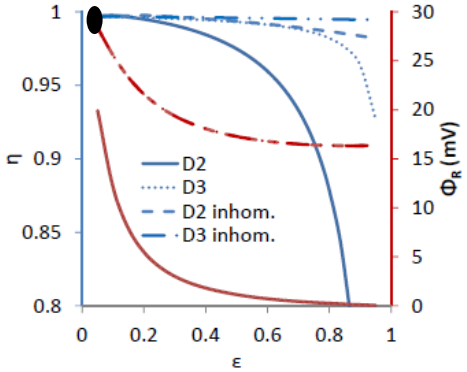

Figure 6. Current efficiency (left axis) and Ohmic voltage drop (right axis) as a function of the ES/MA porosity for design (iii) having no membrane in the pores (D2) or pores only in the outher edge of the ES/MA (inhom.).

Conclusions

A multiphysics model is developed for studying the performance of different photoelectrochemical cells used to electrolyze water and produce hydrogen. The calculated performance of a reference design composed of a multijunction photoactive electrode covered with catalyst on each side and immersed in a conducting water solution is compared with experimental measurements of the ohmic drop in the device which demonstrate acceptable agreement. Geometric variation of the reference device shows that small electrode-separator-assemblies (ESA) are advantageous in regard of the ohmic drop but also lead to significant reductions in current efficiency. Therefore, design options with porous ESAs, perhaps containing proton-conducting membranes, are proposed and compared showing reduced ohmic drops but acceptable efficiency losses for porosities up to 20% compared to the reference case. The influence of convection due to pressure differentials in the device suggest significant reductions in the efficiency already for a small pressure difference (1 mbar pressure difference leads to current efficiencies of 0.97 compared to 1 for neglected convection).

Acknowledgement. This material is based upon work performed by the Joint Center for Artificial Photosynthesis, a DOE Energy Innovation Hub, supported through the Office of Science of the U.S. Department of Energy under Award Number DE-SC0004993.

References

(1) Minggu, L. J.; Daud, W. R.; Kassim, M. B. *Int. J. of Hydrogen Energy*. **2010**, *35*, pp. 5233-5244.
(2) Bak, T.; Nowotny, J.; Rekas, M.; Sorrell, C. C. *Int. J. of Hydrogen Energy*. **2002**, *27*, pp. 991-1022.
(3) Carver, C.; Ulissi, Z.; Ong, C. K.; Dennison, S.; Kelsall, G. H.; Hellgardt, K. *Int. J. of Hydrogen Energy*. **2011**, pp. 1-13.
(4) Nozik, A. J. *Appl Phys Lett*. **1977**, *30*, pp. 567-569.
(5) Kainthla, R. C.; Khan, S. U. M.; Bockris, J. O. M. *Int. J. of Hydrogen Energy*. **2087**, *12*, pp. 381-392
(6) Kelzenberg, M. D.; Turner-Evans, D. B.; Putnam, M. C.; Boettcher, S. W.; Briggs, R. M.; Baek, J. Y.; Lewis, N. S.; Atwater, H. A. *Energy & Environmental Science*, **2011**, *4*, pp. 866-871.
(7) Choi, P.; Bessarabov, D. G.; Datta, R. *Solid State Ionics*, **2004**, *175*, pp. 535-539.